

Development of a new method of wavelet aided trend detection and estimation

Kaz Adamowski,^{1*} Andreas Prokoph² and Jan Adamowski³

¹ University of Ottawa, Ottawa, Ontario, K1N 6N5, Canada

² SPEEDSTAT, 19 Langstrom Crescent, Ottawa, Ontario, K1G 5J5, Canada

³ Massachusetts Institute of Technology, Cambridge, MA, 02139, USA

Abstract:

The detection and estimation of trends in the presence of noise, periodicities, or discontinuous patterns is important in hydrology and climate research studies. The basic idea of currently available trend estimation techniques (tests) is that the trends should be smooth and monotonic; however, hydro-climatologic variables contain multiple signals, and have segments of increasing and decreasing trends. As a result, estimating trends in time series is an essential but arcane art and it is therefore important to continue developing the theory and practice of trend analysis.

In this paper, a new technique is proposed based on the continuous wavelet transform (CWT). CWT permits the transformation of observed time series into wavelet coefficients according to time and scale simultaneously. These coefficients can be used to detect and estimate trends or to reconstruct signals that are of interest. The proposed CWT method was first tested on computer-generated data exhibiting both periodic and noise components. It was then applied to observed monthly minimum streamflow observations extracted from the Reference Hydrometric Basin Network (RHBN) for five different eco-zones in Canada.

It was concluded that the proposed wavelet transform (WT) based method provides a very flexible and accurate tool for detecting and estimating complicated signals. The results from monthly minimum observations indicate that short period fluctuations are decreasing, while multi-annual variability is increasing in Canada. And finally, a persistent ~55-year signal is well correlated with the Pacific Decadal Oscillation in all records, which indicates that trends are not controlled by a single factor. Copyright © 2009 John Wiley & Sons, Ltd.

KEY WORDS wavelet transform; trends; hydrology; streamflow; climate; Canada

Received 9 June 2008; Accepted 15 December 2008

INTRODUCTION

The Earth's climate change is controlled by many factors in addition to greenhouse gases, and there are many different scientific opinions regarding which of these factors is the most significant (Veizer, 2005; Jansen *et al.*, 2007). There are also established linkages between atmospheric circulation, climate and streamflow (Kingston *et al.*, 2006). The climate in general, and climate change in particular, will no doubt remain very difficult to precisely model. There is evidence of past climate variability at various time scales (such as interannual and inter-decadal) at the regional and continental scale (Battarbee *et al.*, 2004), and future changes in variability are highly uncertain.

Many studies indicate that extreme events (such as floods and droughts) are increasing in frequency and/or magnitude (Jansen *et al.*, 2007), but the actual pattern is ambiguous. For example, Kundzewicz *et al.* (2004) analyzed 195 streamflow records for stations all over the world, and found no trends in maximum annual floods. Similar findings of no trends were reported by Zhang *et al.* (2001) for Canadian rivers. Spatial statistical

analysis of the RHBN database indicated that the annual minimum flow had an increasing significant trend for Western Quebec/Southern Ontario, the Mountain-North and Pacific regions, and a decreasing trend for the Central/East region (Adamowski and Bocci, 2001).

For rivers in the United States, Lettenmaier *et al.* (1994) concluded that an increasing trend in streamflows exists for most parts of the USA. However, Douglas *et al.* (2000) found no trends in flood flows, but increasing trends in low flows. Thus different findings have been reported which suggests a large diversity in regional and global climate change interpretations. A prevailing view is that there is an increasing risk of floods and droughts at local or regional scales, and increasing or decreasing water availability at the continental scale (Zhang *et al.*, 2001).

Statistical analysis of observed temperature records worldwide revealed a global increase of 0.3–0.6 °C over the last century (Jansen *et al.*, 2007). Projections of future long-term climate scenarios for Canada estimated a 0.5–1.5 °C temperature increase in southern Canada for the 21st century (Zhang *et al.*, 2000; Bonsal *et al.*, 2001). Almost synchronous with the warming trend, the anthropogenic CO₂ greenhouse gas output increased (Jansen *et al.*, 2007), the population size increased [in particular

* Correspondence to: Kaz Adamowski, University of Ottawa, Ottawa, Ontario, K1N 6N5, Canada. E-mail: adamowsk@eng.uottawa.ca

in urban centers in North America (Karl *et al.*, 1988), and the cosmic ray intensity decreased (Carslaw *et al.*, 2002).

Most reported findings on trends are based on statistical tests for trends. Although many methods have been used for trend detection and testing, none have emerged as standard. Perhaps the most common test for trends is the rank-based nonparametric Mann–Kendall (MK) method. It accepts or rejects the null hypothesis of randomness against the alternative of a monotonic trend. Nonparametric methods do not rely on the estimation of parameters (such as the mean or the standard deviation) describing the distribution of the variable of interest in the population. Mann–Kendall tests are widely used in environmental science because they are simple, robust and can cope with missing values and values below a detection limit. Since the first proposals of the test by Mann (1945) and Kendall (1975), the test was extended in order to include seasonality (Hirsch *et al.*, 1982), multiple monitoring sites (Lettenmaier, 1988), and covariates representing natural fluctuations (Libiseller and Grimvall, 2002). In addition to the studies mentioned earlier, the nonparametric Mann–Kendall test has been used in a variety of climate and streamflow studies in Canada (e.g. Gan, 1995, 1998; Gobena and Gan, 2006). It is, however, well recognized that the MK test is not robust against autocorrelation and cross correlation, and also depends on the sample size as well as magnitude of the trend to be identified. As such, there remains a need for new types of methods in order to detect and test for trends.

In this study a continuous wavelet transform (CWT) based methodology is proposed to extract and reconstruct long-term trends in hydrological data reliably from relatively short records with strong superimposed high frequency (e.g. annual) fluctuations. Wavelet analysis has recently been used to detect interruptions in trends and cycles, as well as to trace rainfall variability (Nakken, 1999), solar irradiance, and interdecadal climate oscillations through time (Lucero and Rodriguez, 2000; Oh *et al.*, 2003). Wavelets are a new class of basic functions that can be very useful for analyzing and interpreting time series data including trends. Kallache *et al.* (2005) used a Discrete Wavelet Transform (DWT) to assess trends in flood data, Partal and Kucuk (2006) used a DWT to assess trends in precipitation data, de Artigas *et al.* (2006) used a DWT to assess trends in geomagnetic activity, and Almasri *et al.* (2008) used a DWT to assess trends in temperature.

The objective of this study was to develop a new test based on the CWT for the detection and identification of

trends in hydrological data at different time-scales and for different climatologic regions.

DATA AND METHODS

Data

The data used in this study are from the Reference Hydrometric Basin Network (RHBN) established by Environment Canada (1999) for detection, monitoring, and assessment of climate change in Canada. These data provide an extraordinary wealth of scientific information for reconstruction and modeling of previous hydrological conditions and their connections to natural and human-caused climate variability. Statistical tests of independence, homogeneity and trends based on the recommendations of Shiau and Condie (1980) have been carried out to verify the quality of the data (Environment Canada, 1999). Canada has been divided into 18 eco-zones based on vegetation, wildlife, latitude, altitude, proximity to oceans, terrain, and other criteria (Environment Canada, 1999).

For this study a computer-simulated hydrological time-series was used as well as the longest and most complete monthly minimum observed flow records representing each of the five southernmost eco-zones in Canada (Pacific Maritime, Montaine Cordillera, Boreal Plain, Mixedwood Plain, and Atlantic Maritime). Minimum monthly flow records were used because the superposition of signals from intra-annual to multi-decadal provided a good opportunity to demonstrate the capability of the trend-extraction method used in this study. In addition these records contain important information on the recurrence pattern of droughts in relation to climatologic forces. The stations from which the data were extracted (Table I) form ~5000 km east-west transect through southern Canada (46–50°N). The rivers that were used in this study are: (1) the Capilano River in British Columbia, (2) the Belly River in Alberta, (3) the Turtle River in Ontario, (4) the Beaurivage River in Quebec, and (5) the Northeast Margaree River in Nova Scotia. These rivers are considered to have remained pristine during the entire recording period.

Signal decomposition using continuous wavelet transform

Time series can be considered as being composed of two different unobserved parts, namely a trend and stochastic component. The detection and estimation of

Table I. River stations used in research

Station	Station Name	Data Interval	Latitude (North)	Longitude (West)	Ecozone
S165	Capilano River above intake	1/1914–12/1996	49.40	123.14	Pacific Maritime
S4	Belly River near Mountain view	10/1911–12/1997	49.10	113.70	Montaine Cordillera
S29	Turtle River near Mine center	7/1914–12/1995	48.85	92.73	Boreal Plain
S244	Beaurivage River at Sainte-Etienne	8/1925–9/1995	46.66	71.29	Mixedwood Plain
S127	NE Margaree River at Margaree Valley	5/1916–12/1996	46.37	60.98	Atlantic Maritime

trend in the presence of stochastic components can be accomplished by wavelet analysis.

Wavelet analysis emerged as a filtering and data compression method in the 1980s (e.g. Morlet *et al.*, 1982). Wavelet analysis transforms a time-series simultaneously in the depth or time domain and scale or frequency domain by using various shapes and sizes of short filtering functions called wavelets. Wavelet transforms (WTs) allow for the automatic localization of periodic-signals, gradual shifts and abrupt interruptions, trends and onsets of trends in time series (Rioul and Vetterli, 1991). WT uses narrow band analysis windows at high frequencies, and wide analysis windows at low frequencies, in contrast to the Sliding-Window Fourier transform that uses shifting analysis windows of constant width. Thus, trend analysis using the proposed CWT method involves separating the trend and stochastic component using wavelet coefficients.

There are two types of WTs, namely discrete (DWT) and continuous (CWT). CWT has the advantage over DWT that all potential scales or frequencies can be analyzed, detected and extracted, while DWT is restricted to a discrete number of scales to be analyzed, mostly multiples of the power of two of the average sampling interval (Rioul and Vetterli, 1991). The advantage of DWT over CWT is that for the scales available, the transform and reconstruction of the signals is perfect while CWT suffers from edge effects. The ability of the CWT to detect, extract, and reconstruct nonlinear long-term trends (e.g. trends with wavelength $>1/2$ of the length of the time-series being analyzed) is pertinent for trend detection in hydrology and climate research, and this was one of the reasons the CWT was chosen for this research.

There are a variety of ‘mother wavelet functions’ that can be used for CWT analysis (e.g. the Morlet wavelet shown in Equation 2), and a variety of ‘mother wavelet functions’ that can be used for DWT analysis (e.g. the Haar wavelet). The mother wavelet function should reflect the type of features present in the time series. For time series with ‘steps’, one would choose a boxcar-like mother wavelet function such as the Haar wavelet (which must be used in conjunction with DWT), while for more smoothly varying time series one would choose a smoother mother wavelet function such as the Morlet wavelet. In this study, the CWT was used with the Morlet wavelet (which can only be used with the CWT) as the mother wavelet function (Morlet *et al.*, 1982) since the Morlet wavelet has been shown to provide robust results in analyses of climate related records (Prokoph and Barthelmes, 1996; Gedalof and Smith, 2001). As well, the influence of edge effects is well defined for the Morlet wavelet, which is useful. (Torrence and Compo, 1998).

The wavelet coefficients W are defined as the power of a signal according to the location (or time) and the scale (or frequency) (Rioul and Vetterli, 1991). The wavelet

coefficients W of a time series $x(s)$ are calculated by a simple convolution

$$W_{\psi}(a, b) = \left(\frac{1}{\sqrt{a}} \right) \int x(s) \psi \left(\frac{s-b}{a} \right) ds \quad (1)$$

where, ψ is the mother wavelet; W_{ψ} are the wavelet coefficients using the mother wavelet; the variable a is the scale factor that determines the characteristic frequency or wavelength; and b represents the translation of the wavelet over $x(s)$ (Chao and Naito, 1995). The bandwidth resolution for a WT varies with $\Delta a = \Delta f = \sqrt{2}/4\pi al$, and a location resolution $\Delta b = al/\sqrt{2}$. Parameter l is used to modify WT bandwidth resolution either in favor of time or in favor of frequency. Note that due to Heisenberg’s uncertainty principle $\Delta f \Delta b = 1/4\pi$, the magnitude of both Δb and Δf cannot be arbitrarily small.

The wavelet coefficients W are normalized to represent the amplitude of Fourier frequencies by replacing \sqrt{a} with a , which allows for a simplified reconstruction of frequency dependent signals. The parameter $l = 6$ for the CWT was chosen, because it has been shown in climate related studies (Ware and Thomson, 2000) to provide a useful compromise between precise resolution in time and frequency for signal analysis. The choice of l depends on the smoothness of the underlying signal. Smooth signals without local discontinuities can be efficiently extracted by using $l = 10$, which retains high scale (or frequency) resolution. For time series that are likely to be characterized by nonstationary and less smooth (i.e. sine-like) periodic signals, it is better to choose a lower value of l (less stretching in time) to maintain a good time resolution. In this study, a value of $l = 6$ was chosen, but testing other values of l (e.g. $l = 2$ to $l = 20$) is suggested for future studies to determine the best value for a particular study.

The shifted and scaled Morlet mother wavelet is defined as

$$\psi_{a,b}^l(s) = \pi^{-\frac{1}{4}} (al)^{-\frac{1}{2}} e^{-i2\pi \frac{1}{a}(s-b)} e^{-\frac{1}{2} \left(\frac{s-b}{al} \right)^2} \quad (2)$$

The relative bandwidth error is constant in all scales and is, for $l = 6$: $\sim 1/6 = 0.16 = 16\%$. The wavelet analysis technique used in this article is explained in detail in Prokoph and Barthelmes (1996).

Due to the fact that one is dealing with finite-length time series, errors will occur at the beginning and end of the wavelet power spectrum, as the Fourier transform assumes the data is cyclic. The wavelet coefficients at the beginning and end of the data set are subject to an ‘edge effect’ because only a half of the Morlet wavelet lies inside the data set. For relatively long wavelengths (e.g. wavelength a covers more than a half of the whole data series), the edge effect approaches zero as soon as the data points cover the complete analysis window. The edge effects are wavelength and location (time) dependent and are higher closer to the ends of the time series than in the middle. This forms a ‘cone of influence’ (Torrence and Compo, 1998) where the calculated wavelet coefficients are unreliable. The

wavelet coefficients in the cone of influence belong predominantly to large scales (low frequencies).

In this study the edge effects were eliminated to take care of unreliable wavelet coefficients in the cone of influence. This was done by dividing the wavelet coefficient of wavelength a extracted from Equation (1) by a standing sine wave of amplitude 1 and wavelength a . The wavelet coefficients as functions of location shift b , scale a , and stretching ratio of wavelet analysis window l , are defined as $W_l(a, b)$. The matrix of the wavelet coefficients $W_l(a, b)$, the so called 'scalogram', was coded with shades of grey for superior graphical interpretation. The wavelet coefficient matrix was sampled at a time resolution to $\Delta b = 1$ month, which allows for simplified reconstruction of periodic signals and trends at the original data interval of the analyzed streamflow data.

The only wavelet coefficients (i.e. amplitudes) and phases that were extracted were those that showed persistently strong magnitudes over time (at least 10% of the average amplitude of the annual cycle, which is always the strongest wavelength). Wavebands that only temporarily exhibit strong signals in the records (i.e. 'events') were not extracted as they are of no consequence for the long-term trend pattern to be reconstructed. Details on the extraction and its accuracy are explained in Prokoph and Patterson (2004).

Reconstruction of periodic components

The original time series can be completely restored (reconstructed) using the inverse WT (Grossmann and Morlet, 1984; Holschneider *et al.*, 1989)

$$x(s) = \int_0^{a \max} \int_0^{b \max} W_a(b) \Psi \left[\frac{(s-b)}{a} \right] db \frac{da}{a^2} \quad (3)$$

where $a \max = 2s$, $b \max = s - 1$, and $W_a(b)$ is the matrix of the wavelet coefficient extracted according to a (scale) and b (time-shift).

In this study the objective was to reconstruct the signals from a small number of wavebands that are essential for trend reconstruction. As such, the reconstruction was reduced to narrow wavebands Δf for a single component centred at a

$$x_a(s) = \int_0^{b \max} W_a(b) \Psi \left[\frac{(s-b)}{a} \right] db \quad (4)$$

with $W_a(b)$ the matrix of the wavelet coefficient extracted according to a (scale) and b (time shift). The reconstruction of a signal $x(s)$ of component a was further simplified by replacing the Morlet wavelet with the Fourier transform. The wavelet coefficient $W_a(b)$ is the modulus of the WT and is set to be the equivalent of a Fourier amplitude. To reconstruct the signal, the phase ϕ of the signal was also extracted from the real and imaginary part of the transform. The inclusion of phase ϕ at each time s for waveband a in the reconstruction equation resulted in

$$x_a(s) = W_a(b) [\cos 2\pi s/a + \phi_a(s)] \quad (5)$$

with a as the frequency (or scale) at time s of the extracted waveband.

To correct for edge effects, calibration coefficients $Y_a(b)$ were determined for each component by calculating the wavelet coefficients of a cosine wave of frequency a and amplitude 1 [$W_{\cos,a}(b)$]. The value of $W_{\cos,a}(b)$ can range between 0.5 (maximum edge effect) and 1 (no edge effect), resulting in the correction coefficient $Y_a(b) = 1/W_{\cos,a}(b)$. This results in

$$x_a(s) = Y_a(b) W_a(b) [\cos 2\pi s/a + \phi_a(s)] \quad (6)$$

Equation 6 is the reconstruction formula used for long-term trend determination of selected wavebands centered around a .

EXAMPLE FROM COMPUTER GENERATED MODEL

A computer generated time series $x(s)$ was created to highlight the extraction and reconstruction capabilities of the proposed methodology. The model consists of 100 equidistant time intervals referred to as 'years' with an 11-year sinusoidal signal with exponentially increasing amplitude. An 11-year cyclicity in the computer generated model was chosen for two reasons: (1) this cycle is long enough to emphasize the influence of edge effects in the cone of influence and the approach of visual correction, and (2) this cycle can be related to the sunspot cyclicity that is considered to partially influence streamflows (Reddy *et al.*, 1989).

High frequency noise resulting in a signal to noise ratio (SNR) of 3:1 was superimposed and strongly diminished the visual detection of the underlying cyclicity (Figure 1A). Wavelet scalograms and phase diagrams permit an easy identification of the 11-year waveband and periodicity in the phase changes, but also show reduced (light grey) wavelet coefficients on the edges at the beginning and end of the record, as well as in the middle (Figure 1B and C).

Figure 1D shows the extracted parameter at $\Delta b = 1$ (year), including the stability of the periodicity (between 10.4 and 11.6 years), the 11-year unit amplitude of the calibration wave, and the amplitude (wavelet coefficient) of the 11-year cycle from the model. The phase changes are gradual with phase jumps from $-\pi$ to $+\pi$ as predetermined by the modeling. The reconstruction of the 11-year component using Equation (6) indicates a good fit to the 11-year model input with the exception of an amplitude between 0 and 20 years, that is too high, and a slight phase shift at 70–100 years. Both of these inaccuracies are predominantly due to the Heisenberg frequency–time uncertainty that affects both the amplitude and phase in the reconstruction. As a result, these remnants of the edge effects indicate that it is important to carefully evaluate the amplitudes of waveband specific trends at both ends of the time series (i.e. by cutting off or neglecting the first and last 10% of the reconstructed signal of the waveband for interpretations).

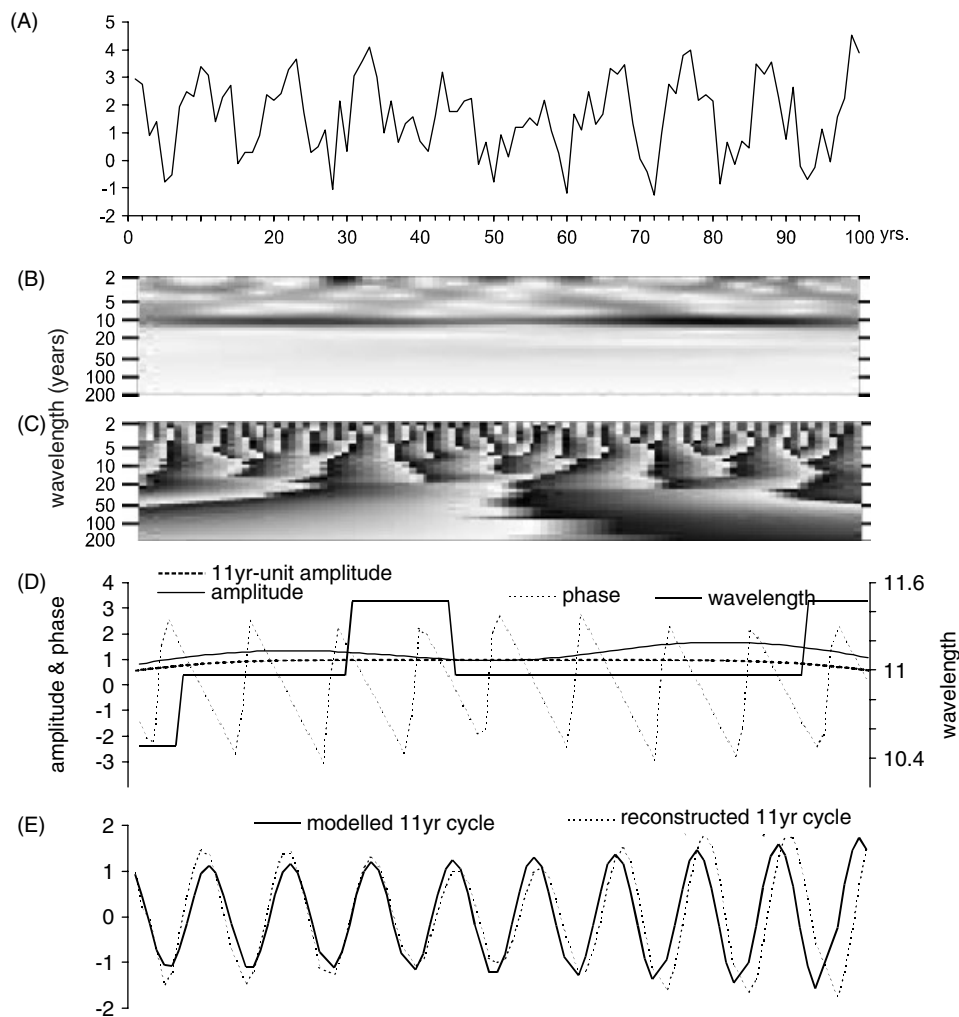


Figure 1. (A) Synthetic 11-year sinusoidal cycle superimposed white noise at SNR of 3/1; (B) Wavelet scalogram using analysis window scale factor $l = 6$ and Morlet wavelet, wavelet coefficient equivalent to Fourier Amplitude (black = maximum, white = 0); (C) Phase diagram from $-p$ (white) to $+p$ (black). Note asymmetry of phase pattern at short wavelength due to noise; (D) Parameter extracted by WT necessary to reconstruct the 9–12-year waveband; (E) Comparison of original modeled 11-year signal and its reconstruction

RESULTS AND DISCUSSION

Data from station S4 of Belly River near Mountain View (Southern Alberta, Canada) extends from November 1911 to December 1997, and provides the most complete and longest record in this study (Figure 2A). Overview WT analysis demonstrated that signals with durations in semi-annual (4–6 months) and annual (10–13 months) wavebands dominated the record (Figure 2B). Less strong and persistent signals of ~ 5 years (4–7 years), ~ 11 years (9–10 years), ~ 22 years (18–25 years), and ~ 55 years (50–65 years) wavebands were superimposed.

The edge-effect corrected wavelet coefficients of these wavebands indicate that the annual signals are about 5 to 7 times, and the semiannual signals about 2 to 5 times, stronger than multi-annual signals (Figure 2C). It is also noticeable that the magnitude of these signals fluctuates over time.

The semiannual and annual signals were reconstructed using Equation 6, and were combined (Figure 2D). This reconstruction of the two signals has a variance of $18.5 \text{ m}^4/\text{s}^2$ and explains 60.3% of the variance of

the original record. This essentially means that the streamflow data mainly exhibit intra-annual and annual oscillations, and relatively fewer interannual or higher oscillations. In Canadian rivers, annual and intra-annual fluctuations dominate the streamflow variability and subdue the underlying trend. Nevertheless, the CWT method efficiently detects and eliminates high frequency variability, in contrast to a pure Fourier transform approach that is unable to remove the temporal variability in the amplitudes of the high frequency fluctuations and to add them to the trend. As a result, the variability that remains in the trend (e.g. the slope of the linear trend) appears small but robust.

In contrast, the Fourier transform requires annual, semiannual, and quarterly wavelengths (Figure 2E) to represent just 52.3% of the original record. In addition, single-window spectral analysis is not capable of extracting trends and other temporal magnitude changes (Davis, 1986).

Wavelet analysis of monthly minimum flow records of four stations from other eco-zones (Table I) indicate that semiannual and annual signals with four weaker

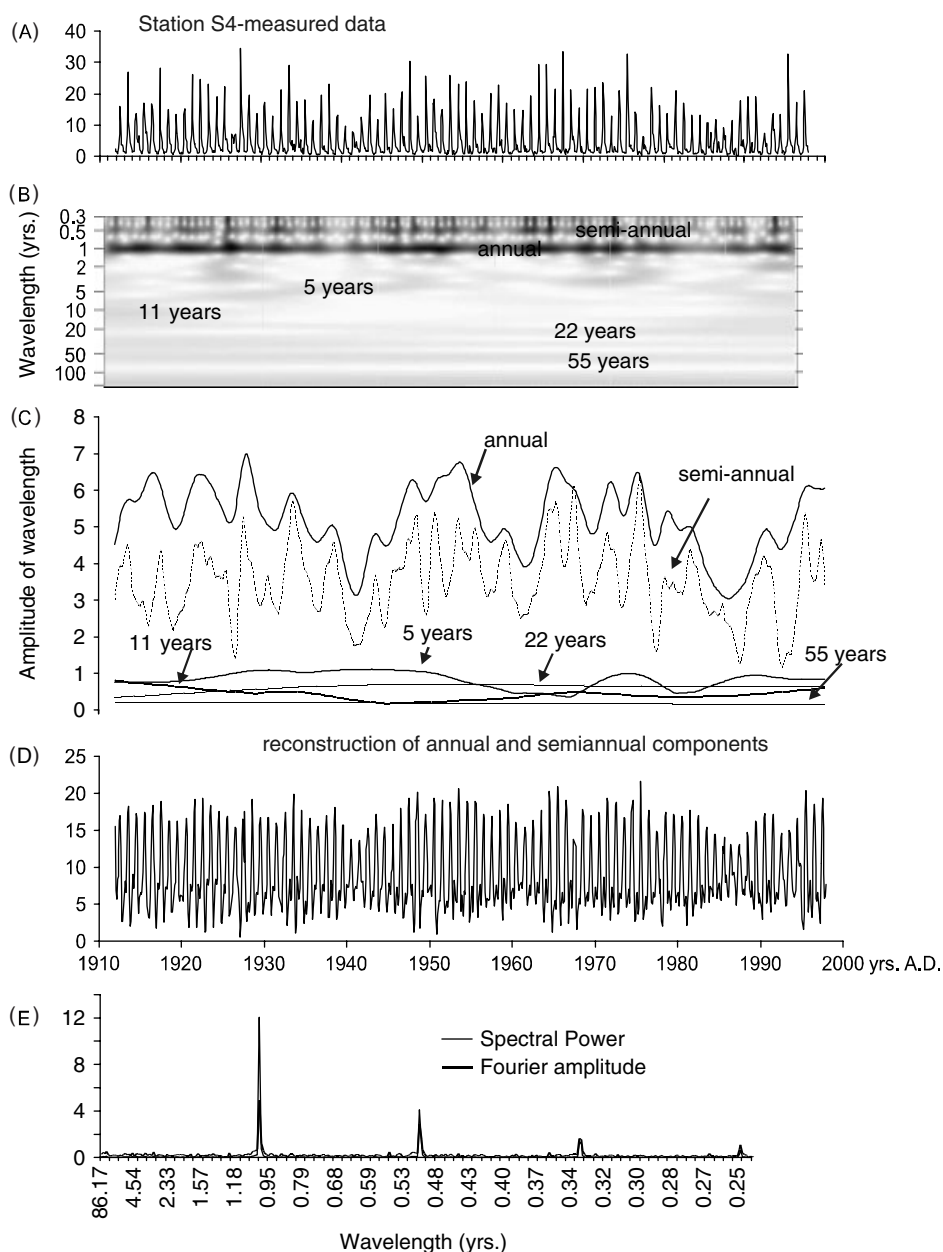


Figure 2. (A) Measured monthly minimum flow data for station 4 (Belly River, Alberta, Canada); (B) Wavelet scalogram (for explanation see Figure 1); (C) Wavelet coefficients (corrected for edge effects) = amplitudes of strongest wavebands; note dominance of annual and semiannual signals; (D) Reconstruction of original dataset using only annual and semiannual components; note temporal variability in amplitude; (E) Power spectrum from same dataset; note that temporal variability cannot be reconstructed and at least four frequencies have to be used to reconstruct the original dataset to obtain the same percentage of variance as two wavelet components

multi-annual wavebands dominate in southern Canada (Figure 3). Additional short-term 'high minimum flow' events (such as in 1927) in station 244, led to short-term spikes in all high frequency wavebands as indicated by the vertical dark grey stripes in the wavelet scalograms (Figure 3). Thus, the same wavebands as for station 4 (Figure 2C) were extracted for reconstruction for the four other stations.

The amplitudes of the semiannual and annual cycles are approximately five times stronger than the multi-decadal cycles, and show similar temporal variability as those from station 4 (Figure 4). In addition, for all stations, the amplitude of the 11-year signal was about twice as high in the 1920s as it was in the 1960s.

Furthermore, the magnitude ratio between the annual and semiannual signal ranges from $\sim 3:2$ in continental ecozones (stations S4, S127), to over $\sim 1:1$ for the Pacific Canada Realm (S165) and the Mixedwood plain along the St. Lawrence River (S244), to $\sim 1:2$ for the Cape Breton peninsula (S127) in Atlantic Canada (Figures 2 and 4).

In this paper, the focus was on extraction and interpretation of linear trends, determined by linear regression of the amplitudes for the interval from 1925 to 1994, that were common for all datasets (Table II). Most of the trends do not appear to be very significant when measured per year compared to the overall variability at each station. For example, a decrease of the amplitude in

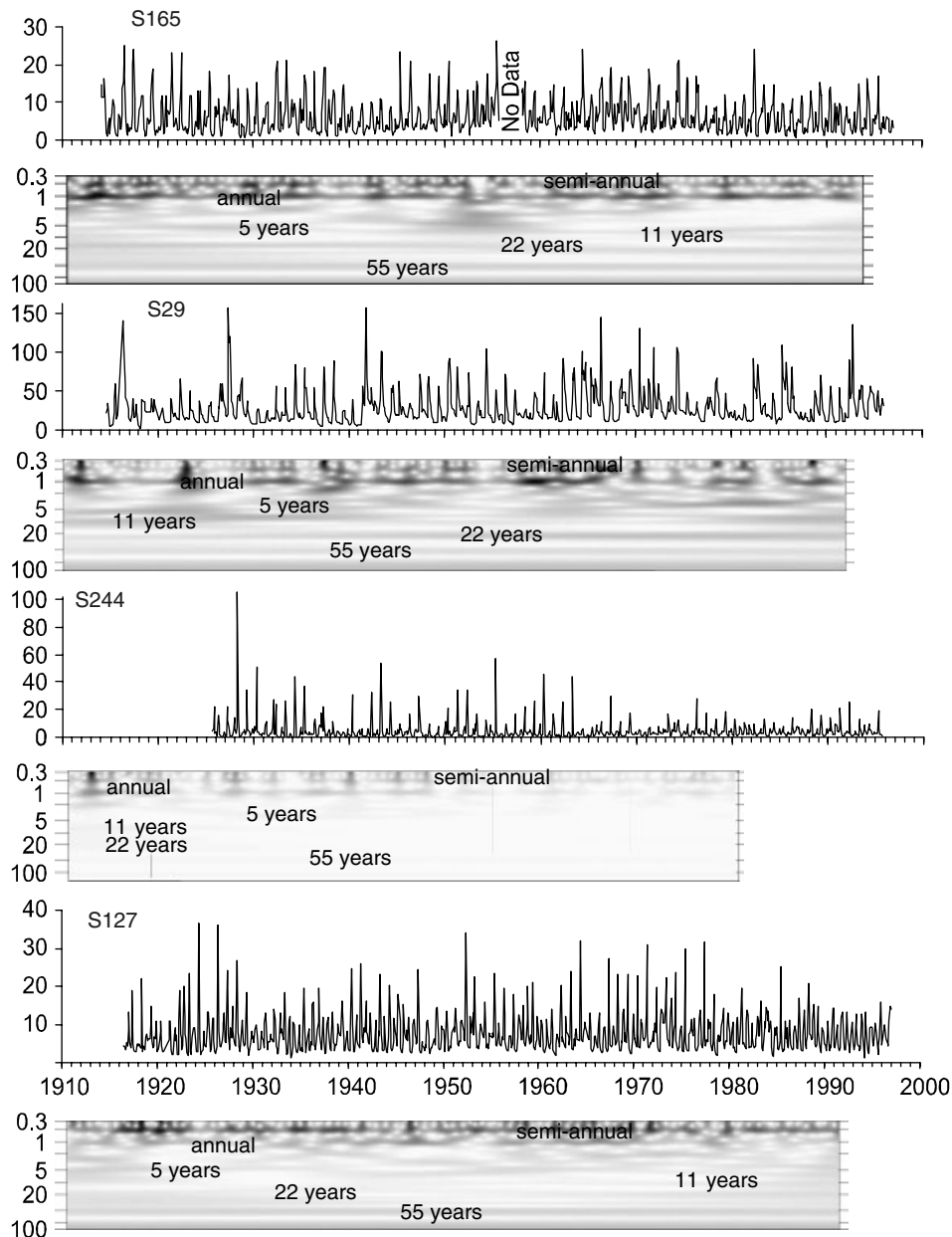


Figure 3. Four monthly minimum flow datasets from the Pacific Coast in the West of Canada (top) to the Atlantic Coast in the East (bottom) with corresponding wavelet scalogram (for explanation see Figure 1)

streamflow related to the 11-year cycle at station S29 of $0.0654 \text{ m}^2/\text{s}/\text{year}$, which is approximately equivalent to a $4.5 \text{ m}^2/\text{s}$ decrease over the ~ 70 -year measurement interval, is $\sim 1\%$ of the extrema of the streamflow increase for this time interval. Consequently, the trend values are similar in their relativity to predicted global warming trends ($\sim 0.5^\circ\text{C}/100$ years), in the presence of extreme regional annual temperature variations of up to 50°C .

For all stations, the linear trend for semiannual and annual variability was found to be decreasing. This indicates that, in general, the seasonality between dryer and less dry periods has decreased over the last century. This means that seasonal droughts cannot be compensated for, by more wet periods during the duration of a year.

The linear trend pattern for multi-decadal cycles is less consistent for different stations (Table II). Regionally,

and for all wavebands, the stations near the Pacific and Atlantic coasts exhibit slightly linear decreasing amplitudes. The Boreal Plain section (S127) in south-central Canada exhibits very strong decreasing linear trends in semiannual and annual variability (Figure 5). However, multi-decadal variability is strongly linearly increasing, which suggests that long periods of droughts were more common at the end of the 20th century than at the beginning.

The 55-year (50–65 year) components for all stations were completely reconstructed from their wavelet coefficients (amplitudes), phases, and wavelengths as given by Equation 6, and compared with meteorological indexes of known multi-decadal variability. Figure 6 shows that all ~ 55 -year cycles from all stations are approximately in phase with each other, with the exception of station 244.

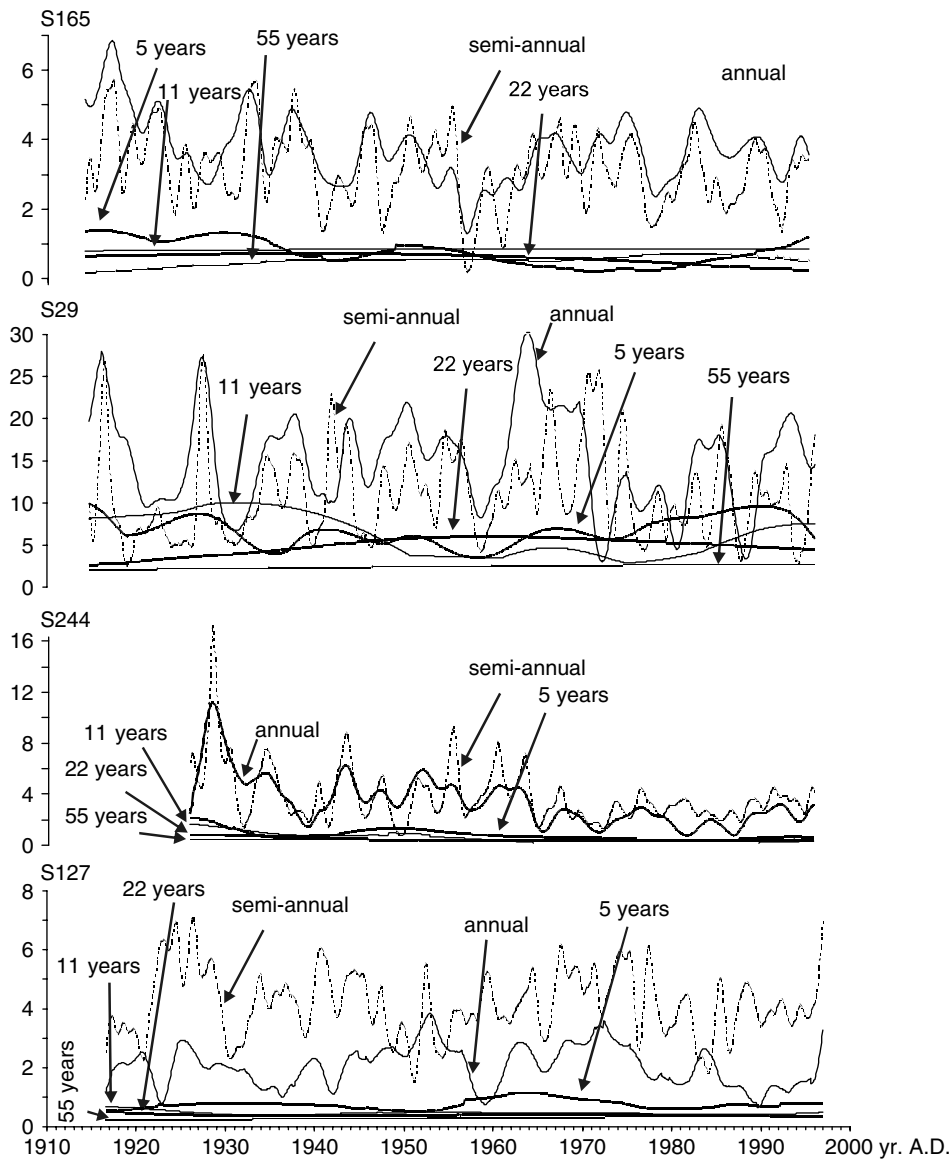


Figure 4. Wavelet coefficients (corrected for edge effects) = amplitudes of strongest wavebands from minimum monthly flow datasets of southern Canada (Figure 3); note changes in the dominance of annual and semiannual signals

Table II. Linear Trends 1925–1994

Station ID	Waveband					
	0.5yr	1yr	5yr	11yr	22yr	55yr
S165	-0.0075	-4.00E-05	-0.0077	0.0031	-0.0072	0.0003
S4	-0.0061	-0.0114	-0.0057	0.0011	0.0001	-0.0005
S29	-0.0105	-0.0389	0.0406	-0.0654	0.0103	0.0086
S244	-0.0438	-0.0661	-0.014	-0.0181	-0.0059	-0.0059
S127	-0.0065	-0.0054	0.0001	0.0001	-8.00E-05	0.0018

Unit: $m^2/(s \cdot years)$

Station 244 is characterized by decreasing amplitude, and thus negative trend, in all wavebands, which is also evident in the obvious drop of large streamflow sessions in the data starting in *ca* 1965. It is possible that the flow of this stream had been influenced by an undocumented natural or anthropogenic event at that time that led to the drop in the flow.

The 55-year minimum monthly flow record from the 55-year waveband varies approximately opposite to the 10-year moving average of the Pacific Decadal Oscillation (PDO) index and to a lesser degree to the North Atlantic Oscillation (NAO) index. In particular, the strong ~ 55 -year ‘monthly minimum flow’ cycle of the Mid-continent station S29 corresponds very well to

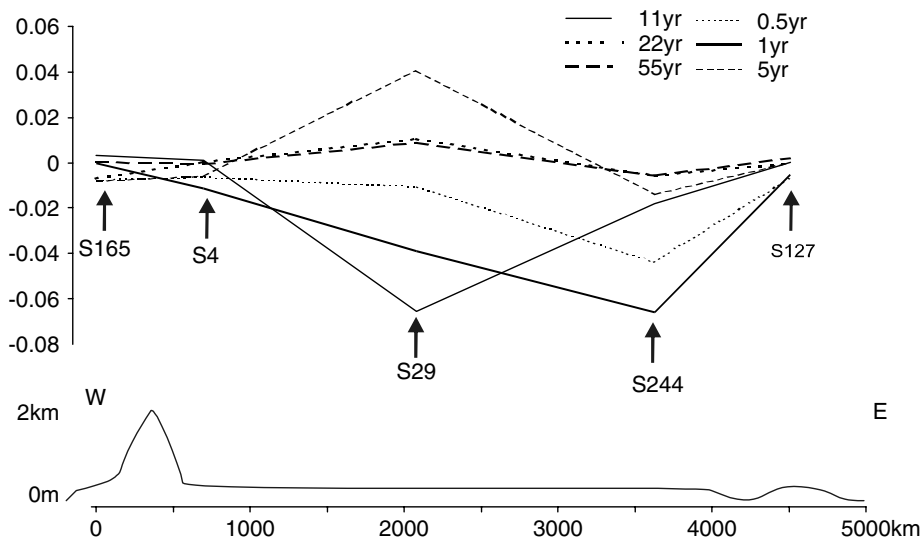


Figure 5. (A) Gradient of linear trend for semiannual to ~55-year wavelet coefficient across Canada; (B) Approximate terrain profile through southern Canada. Note that in general the amplitude (and thus variability) of the signals decrease with the least amount of change close to the coastlines, but that in southcentral Canada there are strong decreases in the amplitudes of the short cycles and some increases in the amplitudes of the longer cycles

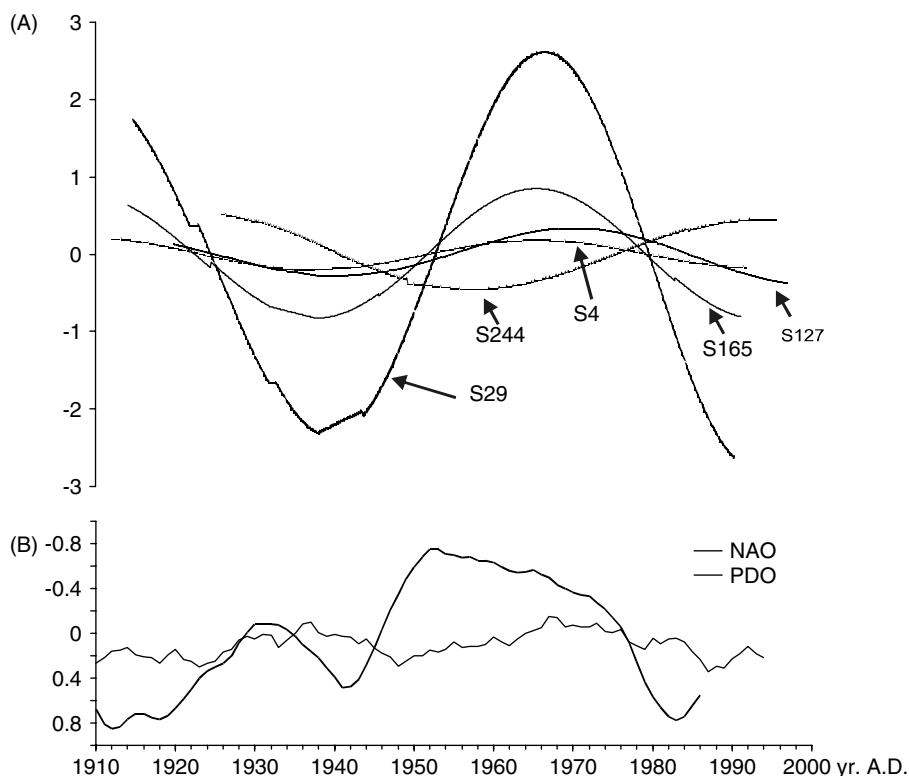


Figure 6. (A) Reconstruction of the 45–60-year signal for five monthly minimum flow datasets; note that with the exception of station S244 the signals are in phase; (B) 10-year moving averages of North Atlantic Oscillation Index (NAO) and Pacific Decadal Oscillation Index (PDO) from Biondi *et al.* (2001). Note that the indices are inverted for visual comparison

the PDO cycle but not to the NAO cycle (Figure 6). Consequently, it is possible that changes in the PDO have a strong influence on the climate and therefore drought and river flows in central Canada. A more comprehensive study that also includes GIS would be necessary to verify the above hypothesis.

In the future, it would be very useful to compare the proposed CWT methodology with other approaches currently used to detect trends. It can be seen from the

results of this study that the proposed CWT methodology does, to a certain degree, enhance the detection of trends which would otherwise be hidden. It should be noted that the robustness of the linear trends of the amplitudes of specific wavebands detected by the CWT method is also related to the time interval over which it is valid (which is ~70 years in this study). For example, the drop in amplitude of $-0.0654 \text{ m}^3/\text{s}/\text{yr}$ relative to extreme events of $\sim 75 \text{ mm}/\text{s}$, is similar to the trend projected for

global warming during the 21st century ($\sim 0.02^\circ\text{C}/\text{yr}$) compared to the extreme annual amplitudes of $\sim 30^\circ\text{C}$ between summer and winter in continental climate zones (Nakicenovic, 2000).

CONCLUSION

A CWT based method was developed and applied to extract waveband specific signals, including long-term trends from hydrological time-series. Testing of the method with a computer generated model showed that nonlinear fluctuating long-term signals can be reliably reconstructed, but that some uncertainty in amplitude, phase, and wavelengths due to Heisenberg's uncertainty principle cannot be avoided. The proposed CWT method is more efficient at reconstructing highly variable time-series from a few wavebands than spectral analysis.

Application of the proposed method to the analysis of minimum monthly flow records from five eco-zones in southern Canada, demonstrated that nonlinear varying high frequency (semiannual and annual) signals can be effectively separated from weaker multi-annual signals. Trend analysis on these signals indicated decreasing seasonality of minimum monthly flow over the last century in southern Canada, while multi-annual variability increased in south-central Canada. Changes in seasonality and in multi-annual variability found in this study are consistent with other reported findings. Several studies have reported a tendency toward decreasing low flows and changes in timing (Hodgkins *et al.*, 2003). Multi-annual variability may reflect several factors such as solar forcing and volcanic activity (Khaliq *et al.*, 2008). Knowledge of changes in seasonality and variability of river flows provides a better understanding of possible impacts (e.g. economic) of climate variability on water resources management.

A reconstructed weak, but persistent ~ 55 -year signal was found to be well-correlated to the PDO. The CWT based methodology presented in this study could be extended to identify climate or anthropogenic forced changes on hydrological systems and to forecast drought or flood trends from hydrological records. It would also be useful to test the use of a variety of different CWT 'mother wavelets' (such as the Mexican Hat wavelet) to assess their effect on the robustness of the proposed CWT method.

ACKNOWLEDGEMENTS

This research was funded by the National Science and Engineering Research Council of Canada (NSERC), Grant RGPIN/007467.

REFERENCES

Adamowski K, Bocci C. 2001. Geostatistical regional trend detection in river flow data. *Hydrological Processes* **15**: 3331–3341.

- Almasri A, Locking H, Shukar G. 2008. Testing for climate warming in Sweden during 1850–1999 using wavelet analysis. *Journal of Applied Statistics* **35**: 431–443.
- Battarbee R, Gasse F, Stickley C. 2004. *Past Climate Variability through Europe and Asia*. Springer: Germany; 638.
- Biondi F, Gershunov A, Cayan DR. 2001. North Pacific decadal climate variability since 1661. *Journal of Climate* **14**: 5–10.
- Bonsal BR, Zhang X, Vincent LA, Hogg WD. 2001. Characteristics of daily and extreme temperatures over Canada. *Journal of Climate* **14**: 1959–1976.
- Carlaw KS, Harrison RG, Kirkby J. 2002. Cosmic rays, clouds, and climate. *Science* **298**: 1732–1737.
- Chao BF, Naito I. 1995. Wavelet analysis provides a new tool for studying Earth's rotation. *EOS* **76**: 164–165.
- Davis JC. 1986. *Statistics and Data Analysis in Geology*. Wiley: New York; 646.
- de Artigas M, Elias A, de Campa P. 2006. Discrete wavelet analysis to assess long-term trends in geomagnetic activity. *Physics and Chemistry of the Earth* **31**: 77–80.
- Douglas EM, Vogel R, Kroll C. 2000. Trends in floods and low flows in the United States: Impact of spatial correlation. *Journal of Hydrology* **240**: 90–105.
- Environment Canada. 1999. *Establishment of the Reference Hydrometric Basin Network (RHBN) for Canada*. Environment Canada: Ottawa; 42.
- Gan T. 1995. Trends in air temperature and precipitation for Canada and North Eastern United States. *International Journal of Climatology* **15**: 1115–1134.
- Gan T. 1998. Hydroclimatic trends and possible climatic warming in the Canadian Prairies. *Water Resources Research* **34**: 3009–3015.
- Gedalof Z, Smith DJ. 2001. Interdecadal climate variability and regime-scale shifts in Pacific North America. *Geophysical Research Letters* **28**: 1515–1518.
- Gobena A, Gan T. 2006. Low-frequency variability in South Western Canadian streamflow: links to large-scale climate anomalies. *International Journal of Climatology* **26**: 1843–1869.
- Grossmann A, Morlet J. 1984. Decomposition of Hardy functions into square integrable wavelets of constant shape. *SIAM Journal on Mathematical Analysis* **15**: 732–736.
- Hirsch R, Slack J, Smith R. 1982. Techniques of trend analysis for monthly water quality data. *Water Resources Research* **18**: 107–121.
- Hodgkins G, Dudley R, Huntington T. 2003. Changes in the timing of high river flows in New England over the 20th century. *Journal of Hydrology* **278**: 244–252.
- Holschneider M, Kronland-Martinet R, Morlet J, Tchamitchian P. 1989. A real-time algorithm for signal analysis with the help of the wavelet transform. In *Wavelet Time-Frequency Methods and Phase Space*, Proceedings of the International Conference, Marseille, France, December 14–18, 1987, Combes J, Grossmann A, Tchamitchian P (eds). Springer-Verlag: Berlin; 286.
- Jansen E, Overpeck J, Briffa KR, Duplessy J-C, Joos F, Masson-Delmotte V, Olago D, Otto-Bliesner B, Peltier WR, Rahmstorf S, Ramesh R, Raynaud D, Rind D, Solomina O, Villalba R, Zhang D. 2007. Paleoclimate. In *Climate Change 2007: The Physical Science Basis*, Contribution of Working Group I to the Fourth Assessment Report of the Intergovernmental Panel on Climate Change, Solomon S, Qin D, Manning M, Chen Z, Marquis M, Averyt KB, Tignor M, Miller HL (eds). Cambridge University Press: Cambridge.
- Kallache M, Rust HW, Kropp J. 2005. Trend assessment: applications for hydrology and climate research. *Nonlinear Processes in Geophysics* **12**: 2001–2210.
- Karl TR, Diaz HF, Kukla G. 1988. Urbanization: its detection and effect in the United States climate record. *Journal of Climate* **1**: 1099–1123.
- Kendall M. 1975. *Rank Correlation Methods*. Charles Griffin: London.
- Khaliq M, Ouarda T, Gachon P, Sushama L. 2008. Temporal evolution of low-flow regimes in Canadian Rivers. *Water Resources Research* **44**: W08436.
- Kingston DG, Lawler DM, McGregor GR. 2006. Linkages between atmospheric circulation, climate and streamflow in the Northern Atlantic: Research prospects. *Progress in Physical Geography* **30**: 143–174.
- Kundzewicz Z, Graczyk D, Przymusinska I, Mauer T, Radziejewski M, Svensson C, Szwed M. 2004. Detection of change in world-wide hydrological time series of maximum annual flow. Technical report: Global Runoff Data Centre.
- Lettenmaier D. 1988. Multivariate nonparametric tests for trend in water quality. *Water Resources Bulletin* **24**: 505–512.
- Lettenmaier DP, Wood EF, Wallis JR. 1994. Hydro-climatological trends in the continental United States. *Water Resources Research* **12**: 1037–1046.

- Libiseller C, Grimvall A. 2002. Performance of partial Mann-Kendall tests for trend detection in the presence of covariates. *Environmetrics* **13**: 71–84.
- Lucero OA, Rodriguez NC. 2000. Statistical characteristics of interdecadal fluctuations in the Southern oscillation and the surface temperature of the equatorial Pacific. *Atmospheric Research* **54**: 87–104.
- Mann H. 1945. Non-parametric tests against trend. *Econometrica* **13**: 245–259.
- Morlet J, Arehs G, Fourgeau I, Giard D. 1982. Wave propagation and sampling theory. *Geophysics* **47**: 203.
- Nakken M. 1999. Wavelet analysis of rainfall-runoff variability isolating climatic from anthropogenic patterns. *Environmental Modelling & Software* **14**: 283–295.
- Nakicenovic N. 2000. *Special Report on Emissions Scenarios: A Special Report of Working Group III of the Intergovernmental Panel on Climate Change*. Cambridge University Press: Cambridge; 599.
- Oh H-S, Ammann CM, Naveau P, Nychka D, Otto-Bliesner BL. 2003. Multi-resolution time series analysis applied to solar irradiance and climate reconstructions. *Journal of Atmospheric and Solar-Terrestrial Physics* **65**: 191–201.
- Partal T, Kucuk M. 2006. Long term trend analysis using discrete wavelet components of annual precipitation measurements in Marmara region (Turkey). *Physics and Chemistry of the Earth* **31**: 1189–1200.
- Prokoph A, Barthelmes F. 1996. Detection of nonstationarities in geological time series: Wavelet transform of chaotic and cyclic sequences. *Computers & Geosciences* **22**: 1097–1108.
- Prokoph A, Patterson RT. 2004. From depth-scale to time-scale: transforming of sediment image color data into high-resolution time-series. In *Image Analysis, Sediments and Paleoenvironments, Developments in Paleoenvironmental Research Series 7*, Francus P (ed.). Springer: Dordrecht; 143–164, Chapter. 8.
- Reddy R, Neralla V, Godson W. 1989. The solar cycle and Indian rainfall. *Journal of Theoretical and Applied Climatology* **39**: 194–198.
- Rioul O, Vetterli M. 1991. Wavelets and signal processing. *IEEE special magazine*, 14–38.
- Shiau SY, Condie R. 1980. *Statistical Tests for Independence, Trend, Homogeneity, and General Randomness*. Environment Canada, Inland Water Directorate: Ottawa.
- Torrence C, Compo GP. 1998. A practical guide to wavelet analysis. *Bulletin of the American Meteorological Society* **79**: 61–78.
- Veizer J. 2005. Celestial climate driver: a perspective from four billion years of the carbon cycle. *Geoscience Canada* **32**: 13–14.
- Ware DM, Thomson RE. 2000. Interannual to multidecadal timescale climate variations in the Northeast Pacific. *Journal of Climate* **13**: 3209–3220.
- Zhang X, Harvey KD, Hogg WD, Yuzyk R. 2001. Trends in Canadian streamflow. *Water Resources Research* **37**: 987–999.
- Zhang X, Vincent LA, Hogg WD, Niitsoo A. 2000. Temperature and precipitation trends in Canada during the 20th century. *Atmosphere-Ocean* **38**: 395–429.